MedChemComm

Accepted Manuscript

ROYAL SOCIETY OF CHEMISTRY

www.rsc.org/medchemcomm

Title: Recognition of diazirine-modified O-GlcNAc by human O-GlcNAcase

Authors: Andrea C. Rodriguez[a] and Jennifer J. Kohler[a]

Abstract

The mammalian O-GlcNAc hydrolase (OGA) removes O-GlcNAc from serine and threonine residues on intracellular glycoproteins. OGA activity is sensitive to N-acyl substitutions to O-GlcNAc, with alkyl diazirine-modified O-GlcNAc (O-GlcNDAz) being completely resistant to removal by OGA. Using homology modeling, we identified OGA residues proximal to the N-acyl position of O-GlcNAc substrate. Mutation of one of these residues, C215, results in mutant enzymes that are able to hydrolytically remove O-GlcNDAz from a model compound. Further, the C215A mutant is capable of removing O-GlcNDAz from a peptide substrate. These results can be used to improve metabolism of O-GlcNAc analogs in cells. In addition, the enzyme specificity studies reported here provide new insight into the active site of OGA, an important drug target.

Introduction

O-linked β-N-acetylglucosamine (O-GlcNAc) is an intracellular form of glycosylation found on a wide range of nuclear and cytoplasmic proteins in most eukaryotes.[1] This post-translational modification of serines and threonines integrates multiple metabolic signals and plays critical roles in cells' ability to respond to changes in nutritional state and other cues.[2] O-GlcNAc is a dynamic modification that, in mammals, is controlled by two enzymes: a single O-GlcNAc transferase (OGT) adds O-GlcNAc to proteins using the UDP-GlcNAc donor,[3] while a single O-GlcNAcase (OGA) hydrolytically removes the modification.[4] O-GlcNAc has critical biological roles, as evidenced by the embryonic lethality of deletion of *Ogt* in mice[5] and by the demonstration that inhibition of OGA activity has protective effects in a mouse model of Alzheimer's disease.[6-9]

While O-GlcNAc modification clearly exerts biological effects at the cellular and organismal levels, much less is known about how O-GlcNAc affects the activity of specific modified proteins. To gain insight into this question, we previously reported a method to introduce the diazirine photocrosslinking group directly on O-GlcNAc residues in living cells (Fig. 1A).[10] In this method, cells engineered to stably express the F383G mutant of UDP-GlcNAc pyrophosphorylase 1 (UAP1) are cultured with a cell-permeable diazirine-modified analog of GlcNAc-1-P (Ac_3GlcNDAz-1-P$(AcSATE)_2$). After entering cells, Ac_3GlcNDAz-1-P$(AcSATE)_2$ is deprotected to GlcNDAz-1-P, which is activated to UDP-GlcNDAz by UAP1(F383G). OGT transfers GlcNDAz from UDP-GlcNDAz to substrate proteins, resulting in O-GlcNDAz residues appearing in place of O-GlcNAc. Subsequent irradiation of cells with UV light yields crosslinking of O-GlcNDAz-modified proteins to neighboring molecules, which can be identified by mass spectrometry-based proteomics methods. Our proposal is that identifying the "proximity interactions"[11] of O-GlcNAc-modified proteins will provide insight into the functional roles of the O-GlcNAc modification.[12]

While characterizing the metabolism of diazirine-modified GlcNAc (GlcNDAz), we noticed that cell lysates overexpressing OGA were incapable of hydrolyzing an O-GlcNDAz mimic.[10] This observation suggested that the O-GlcNDAz modification might accumulate in cells, thereby disrupting the dynamics of O-GlcNAc-ylation. The potential for disruption of OGA activity was concerning, since studies using a non-selective OGA inhibitor *O*-(2-acetamido-2-deoxy-D-glycopyranosylidene)amino-N-phenylcarbamate (PUGNAc) revealed toxicity, including effects on cell cycle progression.[13] However, a more selective OGA inhibitor, 1,2-dideoxy-2′-propyl-α-D-glucopyranoso-[2,1-D]-Δ2′-thiazoline (NButGT), is non-toxic,[14] and OGA inhibition by N-acetyl-D-glucosamine-thiazoline does not prevent cells from progressing through the cell cycle.[15] Based on these precedents, we wondered whether O-GlcNDAz production would be toxic or might affect O-GlcNAc function. In addition, we wished to convert O-GlcNDAz to a reversible modification to ensure that the photocrosslinking approach reports on physiologically normal events.

Here we show that recombinant human OGA is unable to hydrolyze an O-GlcNDAz mimic or to remove O-GlcNDAz from a peptide. Accumulation of the O-GlcNDAz modification in cells causes no overt effects on cellular function, but likely impacts O-GlcNAc dynamics. Thus, we sought to develop a strategy to restore normal O-GlcNAc dynamics to cells producing O-GlcNDAz. We modeled the active site of human OGA based on homology to bacterial N-acetyl-β-glucosaminidases and identified residues in potential conflict with processing of diazirine-modified substrate. We discovered that mutations to C215 resulted in mutant OGA enzymes that could hydrolytically release GlcNDAz from a model substrate. We show that the C215A mutant of OGA can deglycosylate an O-GlcNDAz-modified peptide, offering an approach to restore normal glycosylation dynamics to cells producing O-GlcNDAz. In addition, the results presented here provide new insights into substrate recognition by OGA, an important drug target.

Results

OGA does not hydrolyze an O-GlcNDAz mimic

Previously, we reported that lysate from HeLa cells overexpressing OGA was capable of hydrolyzing an O-GlcNAc mimic, but not an O-GlcNDAz mimic.[10] To confirm that this result was due to OGA substrate specificity, we prepared purified recombinant human OGA for *in vitro* assays (Fig. S1). We measured the substrate tolerance of recombinant OGA, using *p*-nitrophenol derivatives of GlcNAc[4] and GlcNDAz[10] (Fig. 1B). Para-nitrophenol N-acetylglucosamine (*p*NP-GlcNAc) is a mimic of O-GlcNAc that is hydrolyzed by OGA, yielding an increase in absorbance at 405 nm. Similarly, diazirine-modified *p*NP-GlcNAc (*p*NP-GlcNDAz) serves as an O-GlcNDAz mimic and reporter for O-GlcNDAz hydrolysis. As predicted, OGA readily hydrolyzed *p*NP-GlcNAc, while showing no activity toward *p*NP-GlcNDAz (Fig. 1C).

OGA does not remove O-GlcNDAz modification from a peptide

To test directly whether OGA is capable of hydrolytically removing O-GlcNDAz, we assessed the activity of purified recombinant human OGA on a defined O-GlcNDAz-modified peptide. For this experiment, we used a peptide derived from casein kinase II (CKII) containing a single serine residue that is readily O-GlcNAc-modified by OGT.[16] O-GlcNAc- and O-GlcNDAz-modified forms of this peptide were prepared enzymatically. Glycosylated peptides were incubated with OGA and then analyzed by HPLC. We observed that OGA readily hydrolyzed the O-GlcNAc-modified CKII peptide, yielding unmodified CKII peptide, while displaying no activity toward the O-GlcNDAz-modified peptide, which remained intact (Figs. 1D and S2).

O-GlcNDAz production is not toxic

While selective OGA inhibition is non-toxic,[14] other approaches have suggested that disruptions to O-GlcNAc regulatory enzymes can have deleterious effects on cellular homeostasis.[17] Having observed that OGA is incapable of removing the O-GlcNDAz modification, we grew concerned that production of the O-GlcNDAz modification could interfere with O-GlcNAc dynamics and possibly lead to toxic effects. To address this concern, we sought to test whether production of O-GlcNDAz affects cell proliferation or viability. In our strategy for metabolic production of O-GlcNDAz, cells must express a mutant form of the UDP-GlcNAc pyrophosphorylase 1 (UAP1(F383G)) and be cultured in the presence of a cell-permeable, diazirine-modified analog of GlcNAc-1-P (Ac_3GlcNDAz-1-P$(AcSATE)_2$).[10] We compared control HeLa cells to UAP1(F383G)-expressing HeLa cells, HeLa cells cultured with Ac_3GlcNDAz-1-P$(AcSATE)_2$, and UAP1(F383)-expressing HeLa cells cultured with Ac_3GlcNDAz-1-P$(AcSATE)_2$ (*i.e.* O-GlcNDAz-producing cells). When we cultured cells with Ac_3GlcNDAz-1-P$(AcSATE)_2$ for two days, corresponding to the time course of a typical photocrosslinking experiment, we observed no significant effects on cell proliferation (Fig. 2A) or viability (Fig. 2B). We continued culturing cells under these conditions, including a step where we diluted the cells to allow more rapid proliferation. After five days, we observed decreased proliferation of the cells cultured with Ac_3GlcNDAz-1-P$(AcSATE)_2$ (Fig. 2C). However, this effect was not enhanced by expression of UAP1(F383G), which is required for O-GlcNDAz production. In addition, no effects on viability were observed during the longer time course (Fig. 2D). Thus, production of O-GlcNDAz does not have significant effects on the ability of cells to survive and divide during the timeframe of typical photocrosslinking experiments, but Ac_3GlcNDAz-1-P$(AcSATE)_2$ causes slowed cell proliferation under extended conditions.

Modeling the interaction of OGA with O-GlcNDAz

Although O-GlcNDAz production does not have dramatic effects on cell viability or proliferation, it likely alters the dynamics of intracellular protein glycosylation. Our data predict that the O-GlcNDAz modification will accumulate in cells, mimicking the globally elevated O-GlcNAc levels that are observed in some disease states.[2,18] Based on this concern, our goal was to convert O-GlcNDAz from a static modification to a dynamic one. We hypothesized that a small change to the OGA active site might enable activity on diazirine-modified substrates.

While crystal structures of bacterial OGAs in complex with inhibitors have been solved,[19,20] structural information about mammalian OGAs has come solely from modeling.[21] As noted by others,[19,21,22] *Clostridium perfringens* OGA and *Bacteriodies thetaiotaomicron* OGA are closely related to human OGA: sequence alignment using Basic Local Alignment Search Tool (BLAST)[23] reveals that *Clostridium perfringens* OGA displays 51% similarity to human OGA, while *Bacteriodies thetaiotaomicron* is 55% similar to human OGA. Both bacterial enzymes have aspartates at positions corresponding to D174 and D175 of human OGA, identified as catalytic residues in the human enzyme.[24]

We used the Protein Homology/analogY Recognition Engine V 2.0 (PHYRE^2; http://www.sbg.bio.ic.ac.uk/phyre2) remote homology modeling server[25] to create a model of human OGA. This model was aligned with the structure of *C. perfringens* OGA solved in complex with PUGNAc (PDB: 2CBJ)[19] (Fig. 3A) and with the structure of *B. thetaiotaomicron* solved in complex with Thiamet G (PDB: 2VVN)[20] (Fig. 3B). Using these alignments, we identified OGA residues proximal to the nitrogen attached to the C-2 position of the pyranose ring of each inhibitor. We constructed plasmids encoding OGA with each of the following mutations: F214A, C215A, L248G, T250A, W278A, and W278F, although the W278A mutant failed to express at detectable levels (Fig. S3A). *E. coli* lysates overexpressing each OGA mutant were incubated with *p*NP-GlcNAc or *p*NP-GlcNDAz and production of *p*-nitrophenol was detected by monitoring absorbance at 405 nm. Only lysate overexpressing the C215A mutant produced significant hydrolysis of both *p*NP-GlcNAc and *p*NP-GlcNDAz (Fig. S3B and S3C). Based on this result, we constructed an additional OGA mutant in which C215 was mutated to glycine (C215G) based on the idea that additional space at this position might better accommodate hydrolysis of diazirine-modified substrate.

Mutations to OGA residue C215 confer activity toward an O-GlcNDAz mimic

Next, we assessed the activity of purified OGA(C215A) and OGA(C215G) (Fig. S1) toward a diazirine-modified substrate. We measured the kinetics of *p*NP-GlcNAc and *p*NP-GlcNDAz hydrolysis by wild-type OGA or mutant OGA using a continuous assay that measures *p*-nitrophenol production. Wild-type OGA readily hydrolyzed the *p*NP-GlcNAc substrate (Fig. 3C). Kinetic parameters for this reaction were similar to reported values,[26 27] confirming the reliability of the continuous assay measurements. Both the C215A and C215G mutants retained activity toward *p*NP-GlcNAc, displaying catalytic efficiencies (k_{cat}/K_m) 2- to 3-fold lower than the wild-type enzyme. In the case of the C215G mutant, this was achieved by modest increases in both k_{cat} and K_m. Both the C215A and C215G mutants also hydrolyzed *p*NP-GlcNDAz (Fig. 3D). Remarkably, the catalytic efficiency for the C215A mutant hydrolyzing *p*NP-GlcNDAz was comparable to the catalytic efficiency for wild-type OGA acting on *p*NP-GlcNAc, although the k_{cat} and K_m values for the C215A/*p*NP-GlcNDAz pair were about 6-fold lower than those for the wild-type/*p*NP-GlcNAc pair. Overall, the kinetic analysis showed that both the C215A and C215G mutants of OGA are capable of efficient hydrolysis of *p*NP-GlcNDAz.

C215A mutant of OGA can remove O-GlcNDAz from a peptide substrate

Next, we examined whether the C215A mutation to OGA conferred the ability to hydrolytically remove O-GlcNDAz from a peptide. O-GlcNDAz-ylated CKII peptide was prepared enzymatically and purified by HPLC. The purified O-GlcNDAz-ylated peptide was incubated with wild-type OGA or the C215A mutant, and the reaction products were analyzed by HPLC (Figs. 4 and S6). Whereas wild-type OGA failed to hydrolyze O-GlcNDAz, the C215A mutant was active, as indicated by loss of the peak corresponding to O-GlcNDAz-ylated peptide and appearance of new peak corresponding to unmodified peptide. Under these conditions, approximately 37% of the O-GlcNDAz-modified peptide was deglycosylated, which compares favorably to the deglycosylation of O-

GlcNAc-modified peptide by wild-type OGA, in which 53% of the peptide was deglycosylated (Fig. 1D). Thus, O-GlcNDAz becomes a reversible post-translational modification in the presence of the C215A mutant of OGA.

Conclusions

Here we examined the activity of recombinant human OGA toward substrates in which the N-acyl side chain of GlcNAc is extended by modification with an alkyl diazirine (GlcNDAz). Vocadlo and co-workers have shown that human OGA is relatively accommodating of steric bulk at the N-acyl position;[26] however, the alkyl diazirine modification is larger than the substituents they evaluated. Thus, it is perhaps unsurprising that we found that wild-type OGA fails to hydrolytically remove GlcNDAz from either *p*-nitrophenol or a peptide. To interpret these results molecularly, we turned to a structural model of human OGA constructed by homology modeling. We examined the model in alignment with bacterial OGAs complexed with inhibitors that are structural analogs of the substrate. This analysis revealed the potential for steric clashes between the diazirine modification and a handful of amino acid side chains projecting into the enzyme active site. In particular, the N-acyl methyl group on the inhibitor PUGNAc projects toward the C215 side chain of OGA, with a C-S separation of about 4 Å. Mutations to C215 had little effect on the rate of *p*NP-GlcNAc hydrolysis, suggesting that this amino acid chain does not play a significant role in catalysis. As predicted, mutation of this position to a smaller side chain (alanine or glycine) enabled activity on diazirine-modified substrates, consistent with the idea that there is a steric conflict between the cysteine side chain and the diazirine modification. Mutations to other nearby amino acid positions resulting in dramatically reduced activity toward *p*NP-GlcNAc, suggesting that these positions may be critical for catalysis or proper enzyme folding. Thus, the homology model served as a predictive tool that enabled us to reengineer the enzyme active site to optimize enzyme-substrate recognition. In the absence of an available crystal structure of human OGA, homology modeling may also be employed in efforts to design new OGA inhibitors.

The observation that OGA is unable to remove the O-GlcNDAz modification has important implications for our recently reported method for discovering interaction partners of O-GlcNAc-modified proteins. This photocrosslinking method relies on metabolic production of O-GlcNDAz. Since OGA fails to remove O-GlcNDAz, we predict that the modification will accumulate in cells, raising the overall level of intracellular protein glycosylation. Because inhibition of OGA was reported to cause slowed proliferation and cell cycle defects,[13] we measured the proliferation and viability of O-GlcNDAz-producing cells. We observed no dramatic effects attributable to O-GlcNDAz production, consistent with a growing recognition that selective OGA inhibition is non-toxic.[14,28] Nonetheless, we recognize that more subtle effects may not be detected in proliferation and viability assays. Indeed, the half-life of O-GlcNAc modification varies for different proteins,[29,30] with O-GlcNAc dynamics playing a critical role for some functions.[31] Thus, we searched for OGA mutants capable of removing O-GlcNDAz. Our discovery that mutations to C215 of OGA confer activity toward diazirine-modified substrates offers a strategy for improving our O-GlcNDAz crosslinking method. By introducing expression of OGA(C125A) into O-GlcNDAz producing cells, we envision restoring the normal dynamics of intracellular protein glycosylation to enable the photocrosslinking method to accurately report on physiologically relevant interactions in which O-GlcNAc plays a critical role.

Experimental Procedures

Cell culture

Parental HeLa cells were obtained from ATCC. HeLa cells stably expressing UAP1(F383G) cells were described previously.[10]

Chemicals

Diazirine-modified 4-nitrophenyl-N-acetylglucosamine (*p*NP-GlcNDAz) and diazirine-modified UDP-GlcNAc (UDP-GlcNDAz) were prepared as described previously[10] and dissolved in DMSO. 4-nitrophenol-N-acetylglucosamine (*p*NP-GlcNAc) was obtained from Sigma (N9376).

Toxicity analysis

Parental HeLa cells or HeLa cells expressing UAP1(F383G) were cultured in DMEM containing 5% FBS and 1% penicillin/streptomycin. Initial conditions were 2 million cells in 10 mL of media in a 10-cm tissue culture plate. After 24 h and 48 h, 100 μM of Ac_3GlcNDAz-1-P(Ac-SATE)$_2$ in DMSO or DMSO alone was added to the cell media.[10] For the short time course, cell number and viability were determined at 72 h, using the Invitrogen Countess automated cell counter according to the manufacturer's instructions. For the long time course, cells were diluted at 72 h to 2 million cells in 10 mL of media (containing Ac_3GlcNDAz-1-P(Ac-SATE)$_2$ in DMSO or DMSO alone) in a 10-cm tissue culture plate. Additional Ac_3GlcNDAz-1-P(Ac-SATE)$_2$ in DMSO or DMSO alone was added at 96 h and 120 h. At 144 h, cell number and viability were determined using the Invitrogen Countess automated cell counter according to the manufacturer's instructions.

Expression and purification of recombinant human OGA

A pBAD/HisA plasmid encoding OGA[32] was used to transform TOP-10 *E. coli*. A single colony was added to a 5-mL starter culture of LB media containing with 50 μg/mL ampicillin and cultured overnight at 37 °C with shaking. The entire starter culture was used to inoculate a 500-mL culture of LB media containing with antibiotics, which was then cultured at 37 °C with shaking until the OD_{600} reached 0.8. The culture was cooled to room temperature, then induced at 0.02% arabinose by culturing overnight at 20 °C with shaking. Bacteria were lysed in 50 mM sodium phosphate buffer pH 7.8, containing 500 mM NaCl, 10 mM imidazole, 0.1% Tween-20, and 0.2 mM PMSF. Sonication was performed at 4 °C for 10 min with alternate cycling between 5 sec of sonication and 8 sec recovery. Insoluble material was removed by centrifugation (15,000*g*, 4 °C, 30 min). For in-lysate assays, OGA mutant overexpression was assessed by immunoblot using an antibody that recognizes the hexahistidine affinity tag (Sigma Aldrich, H1029). For experiments with purified protein, the supernatant was applied to a Profinia IMAC column. Purification and desalting were performed using the Bio-Rad Profinia system with recommended buffers. Recombinant OGA mutant proteins were prepared by the same method.

Expression and purification of recombinant human OGT

A pET24b plasmid encoding OGT[33] was used to transform BL21(DE3) *E. coli*. A single colony was added to a 50-mL culture of LB media with 50 μg/mL kanamycin, which was incubated at 37 °C overnight without shaking. Eight mL of this culture was used to inoculate a 1-L culture of LB containing ampicillin, which was incubated at 37 °C with shaking until the OD_{600} reached 0.6 - 0.8. After cooling to 20 °C for 1 h, cells were induced by adding 0.5 mM IPTG, then incubated overnight at 20 °C with shaking. After harvesting by centrifugation, cells were lysed in 50 mM Tris-HCl pH 7.5 containing 500 mM NaCl, 1% Triton X-100, 20 mM β-mercaptoethanol, 0.3 mg/mL fresh lysozyme, and 1/50 dilution of protease inhibitor cocktail (Sigma, S8830; contains pancrease extract, thermolysin, chymotrypsin, trypsin, bestain HCl, pepstatin A and papain). Lysates were incubated on ice for 30 min, then sonicated at 4 °C for 5 min, alternating 10 sec sonication with 30 sec recovery. After removing insoluble material by centrifugation (15,000*g*, 4 °C, 30 min), the supernatant was applied to Ni-NTA resin. Resin was washed with 300 mL of 20 mM Tris-HCl buffer pH 7.5, containing 500 mM NaCl, 20 mM β-mercaptoethanol, 0.1 mM PMSF. Then, 50 mL of the same buffer, with the addition of 200 mM imidazole, was used to elute OGT from the resin.

Kinetic analysis

Recombinant OGA or OGA mutant was incubated in 50 mM sodium cacodylate buffer pH 6.5, containing 5 mg/mL BSA and 4 mM GalNAc. *p*NP-GlcNAc or *p*NP-GlcNDAz was added to achieve the indicated concentration. For *p*NP-GlcNAc reactions, the enzyme concentration was 50 nM; for *p*NP-GlcNDAz reactions, enzyme concentration was 250 nM. Reactions (100 μL total volume) were performed in a 96-well clear flat bottom plate. Reaction progress was monitored with a Synergy Neo plate reader at 405 nm. Hydrolytic release of *p*-nitrophenol yields an increase in absorbance at 405 nm. Because *p*-nitrophenolate has a stronger absorbance than *p*-nitrophenol, reactions are typically quenched with base to achieve maximal signal. However, we desired a continuous assay measuring enzyme activity at pH 6.5, so we could not perform measurements at a basic pH. Instead, we carefully controlled the pH of all reactions and calibrated values relative to a *p*-nitrophenol standard also measured at pH 6.5, in a manner similar to other reports describing the use of 4-nitrophenol reporters.[27,34-36] Indeed Hayre *et al.* demonstrated accurate determination of kinetics of sialidase-catalyzed reactions using a *p*-nitrophenol reporter and continuous absorbance measurements at pH 6.0.[34] Although the reaction buffer was at a pH lower than the pK_a of 4-nitrophenol, a substantial increase in absorbance was detectable when OGA activity was present. Changes in

absorbance at 405 nm were linear with respect to time over the period between 5 and 35 minutes (Figs. S4 and S5). These data were used to determine initial rates, which were plotted versus substrate concentration (Fig. 3C and D). Michaelis-Menten parameters were calculated using GraphPad Prism and are presented in Table 1.

Enzymatic synthesis of O-GlcNAc-ylated and O-GlcNDAz-ylated peptides

CKII peptide (Ac-YPGGSTPVSSANMM-NH_2; 100 μM; obtained from Genescript,) and UDP-GlcNAc or UDP-GlcNDAz (500 μM) were reacted with recombinant OGT (1 μM) in 20 mM Tris-HCl buffer pH 8.0, containing 12.6 mM $MgCl_2$ and 20 mM β-mercaptoethanol. The reaction mixture was incubated for 16 h at 37 °C. Modified peptide was then purified by HPLC using an XDB-phenyl column, as described.[10] Solvent was removed by rotary evaporation.

Peptide deglycosylation by OGA

Glycosylated (O-GlcNAc or O-GlcNDAz) peptide was incubated with 750 nM OGA (wild-type or C215A) in 50 mM sodium cacodylate buffer pH 6.5, containing 4 mM GalNAc for 20 h at room temperature. Reactions mixtures were heated at 100 °C for 5 min to denature OGA, then analyzed by HPLC using an XDB-phenyl column and UV detection at 220 nm, as described.[10] Peaks were collected from the HPLC and analyzed by intact mass measurement via electrospray ionization-quadruple time of flight (ESI-QTOF) to confirm peptide identities. From the reaction mixture containing O-GlcNDAz-modified CKII treated with wild-type OGA, the major peak had similar mobility to O-GlcNDAz-modified CKII and yielded an observed mass (1732 Da) corresponding to O-GlcNDAz-ylated CKII peptide (predicted 1728 Da). From the reaction mixture containing O-GlcNDAz-modified CKII treated with OGA(C215A), the major peak had mobility identical to unmodified CKII and yielded an observed mass (1461 Da) most consistent with deglycosylated CKII peptide (predicated 1440 Da).

Acknowledgements

We thank Dr. John Hanover (NIDDK) for the pBAD/HisA OGA plasmid, Dr. Kate Harwood (NIDDK) for advice on OGA purification, Dr. Suzanne Walker (Harvard Medical School) for the pET24b OGT plasmid, Dr. Ilmin Kwon (UT Southwestern) for advice on OGT purification, Dr. Kenneth Westover (UT Southwestern) for the use of the Profinia system, and Dr. David Vocadlo (Simon Frasier), Suong Nguyen (UT Southwestern), and Dr. Seok-Ho Yu (Complex Carbohydrate Research Center) for insightful discussions. We acknowledge support from the Welch foundation (I-1686), the NIH (R01GM090271 and T32GM007062), and Graduate Programs Initiative from the UT System.

Notes and references

[a] Department of Biochemistry, University of Texas Southwestern Medical Center, Dallas, TX 75390-9038

Electronic Supplementary Information (ESI) available: pdf containing Supplementary Figures 1-6; pdb file containing coordinates for homology model of human OGA. See DOI: 10.1039/b000000x/

1. J. Ma and G. W. Hart, *Clin. Proteomics*, 2014, **11**, 8.
2. M. R. Bond and J. A. Hanover, *Ann. Rev. Nutr.*, 2013, **33**, 205–229.
3. R. S. Haltiwanger, G. D. Holt, and G. W. Hart, *J. Biol. Chem.*, 1990, **265**, 2563–2568.
4. D. L. Dong and G. W. Hart, *J. Biol. Chem.*, 1994, **269**, 19321–19330.
5. R. Shafi, S. P. N. Iyer, L. G. Ellies, N. O'Donnell, K. W. Marek, D. Chui, G. W. Hart, and J. D. Marth, *Proc. Natl. Acad. Sci. U. S. A.*, 2000, **97**, 5735–5739.
6. S. A. Yuzwa, X. Shan, M. S. Macauley, T. Clark, Y. Skorobogatko, K. Vosseller, and D. J. Vocadlo, *Nat. Chem. Biol.*, 2012, **8**, 393–399.
7. Y. Yu, L. Zhang, X. Li, X. Run, Z. Liang, Y. Li, Y. Liu, M. H. Lee, I. Grundke-Iqbal, K. Iqbal, D. J. Vocadlo, F. Liu, and C.-X. Gong, *PLoS ONE*, 2012, **7**, e35277.
8. D. L. Graham, A. J. Gray, J. A. Joyce, D. Yu, J. O'Moore, G. A. Carlson, M. S. Shearman, T. L. Dellovade, and H. Hering, *Neuropharmacology*, 2014, **79**, 307–313.
9. P. Borghgraef, C. Menuet, C. Theunis, J. V. Louis, H. Devijver, H. Maurin, C. Smet-Nocca, G. Lippens, G. Hilaire, H. Gijsen, D. Moechars, and F. Van Leuven, *PLoS ONE*, 2013, **8**, e84442.
10. S.-H. Yu, M. Boyce, A. M. Wands, M. R. Bond, C. R. Bertozzi, and J. J. Kohler, *Proc. Natl. Acad. Sci. U. S. A.*, 2012, **109**, 4834–4839.
11. E. N. Firat-Karalar, N. Rauniyar, J. R. Yates III, and T. Stearns, *Curr. Biol.*, 2014, **24**, 664–670.
12. B. Li and J. J. Kohler, *Traffic*, 2014, **15**, 347–361.

13. C. Slawson, N. E. Zachara, K. Vosseller, W. D. Cheung, M. D. Lane, and G. W. Hart, *J. Biol. Chem.*, 2005, **280**, 32944–32956.
14. M. S. Macauley, A. K. Bubb, C. Martinez-Fleites, G. J. Davies, and D. J. Vocadlo, *J. Biol. Chem.*, 2008, **283**, 34687–34695.
15. C. Slawson, T. Lakshmanan, S. Knapp, and G. W. Hart, *Mol. Biol. Cell*, 2008, **19**, 4130–4140.
16. L. K. Kreppel and G. W. Hart, *J. Biol. Chem.*, 1999, **274**, 32015–32022.
17. O. Sekine, D. C. Love, D. S. Rubenstein, and J. A. Hanover, *J. Biol. Chem.*, 2010, **285**, 38684–38691.
18. H.-B. Ruan, J. P. Singh, M.-D. Li, J. Wu, and X. Yang, *Trends Endocrinol. Metab.*, 2013, **24**, 301–309.
19. F. V. Rao, H. C. Dorfmueller, F. Villa, M. Allwood, I. M. Eggleston, and D. M. F. van Aalten, *EMBO J.*, 2006, **25**, 1569–1578.
20. S. A. Yuzwa, M. S. Macauley, J. E. Heinonen, X. Shan, R. J. Dennis, Y. He, G. E. Whitworth, K. A. Stubbs, E. J. McEachern, G. J. Davies, and D. J. Vocadlo, *Nat. Chem. Biol.*, 2008, **4**, 483–490.
21. N. A. N. de Alencar, P. R. M. Sousa, J. R. A. Silva, J. Lameira, C. N. Alves, S. Martí, and V. Moliner, *J. Chem. Inf. Model.*, 2012, **52**, 2775–2783.
22. R. J. Dennis, E. J. Taylor, M. S. Macauley, K. A. Stubbs, J. P. Turkenburg, S. J. Hart, G. N. Black, D. J. Vocadlo, and G. J. Davies, *Nat. Struct. Mol. Biol.*, 2006, **13**, 365–371.
23. M. Johnson, I. Zaretskaya, Y. Raytselis, Y. Merezhuk, S. McGinnis, and T. L. Madden, *Nucl. Acids. Res.*, 2008, **36**, W5–9.
24. N. Cetinbaş, M. S. Macauley, K. A. Stubbs, R. Drapala, and D. J. Vocadlo, *Biochemistry*, 2006, **45**, 3835–3844.
25. L. A. Kelley and M. J. E. Sternberg, *Nat. Protoc.*, 2009, **4**, 363–371.
26. M. S. Macauley, G. E. Whitworth, A. W. Debowski, D. Chin, and D. J. Vocadlo, *J. Biol. Chem.*, 2005, **280**, 25313–25322.
27. M. S. Macauley, J. Chan, W. F. Zandberg, Y. He, G. E. Whitworth, K. A. Stubbs, S. A. Yuzwa, A. J. Bennet, A. Varki, G. J. Davies, and D. J. Vocadlo, *J. Biol. Chem.*, 2012, **287**, 28882–28897.
28. M. S. Macauley and D. J. Vocadlo, *Biochim. Biophys. Acta*, 2010, **1800**, 107–121.
29. E. P. Roquemore, M. R. Chevrier, R. J. Cotter, and G. W. Hart, *Biochemistry*, 1996, **35**, 3578–3586.
30. C. F. Chou, A. J. Smith, and M. B. Omary, *J. Biol. Chem.*, 1992, **267**, 3901–3906.
31. J. E. Rexach, P. M. Clark, D. E. Mason, R. L. Neve, E. C. Peters, and L. C. Hsieh-Wilson, *Nat. Chem. Biol.*, 2012, **8**, 253–261.
32. E. J. Kim, D. O. Kang, D. C. Love, and J. A. Hanover, *Carbohydr. Res.*, 2006, **341**, 971–982.
33. M. B. Lazarus, Y. Nam, J. Jiang, P. Sliz, and S. Walker, *Nature*, 2011, **469**, 564–567.
34. J. K. Hayre, G. Xu, L. Borgianni, G. L. Taylor, P. W. Andrew, J.-D. Docquier, and M. R. Oggioni, *BMC Biochem.*, 2012, **13**, 19.
35. H. Paritala and K. S. Carroll, *Anal. Biochem.*, 2013, **440**, 32–39.
36. O. Tabachnikov and Y. Shoham, *FEBS J.*, 2013, **280**, 950–964.

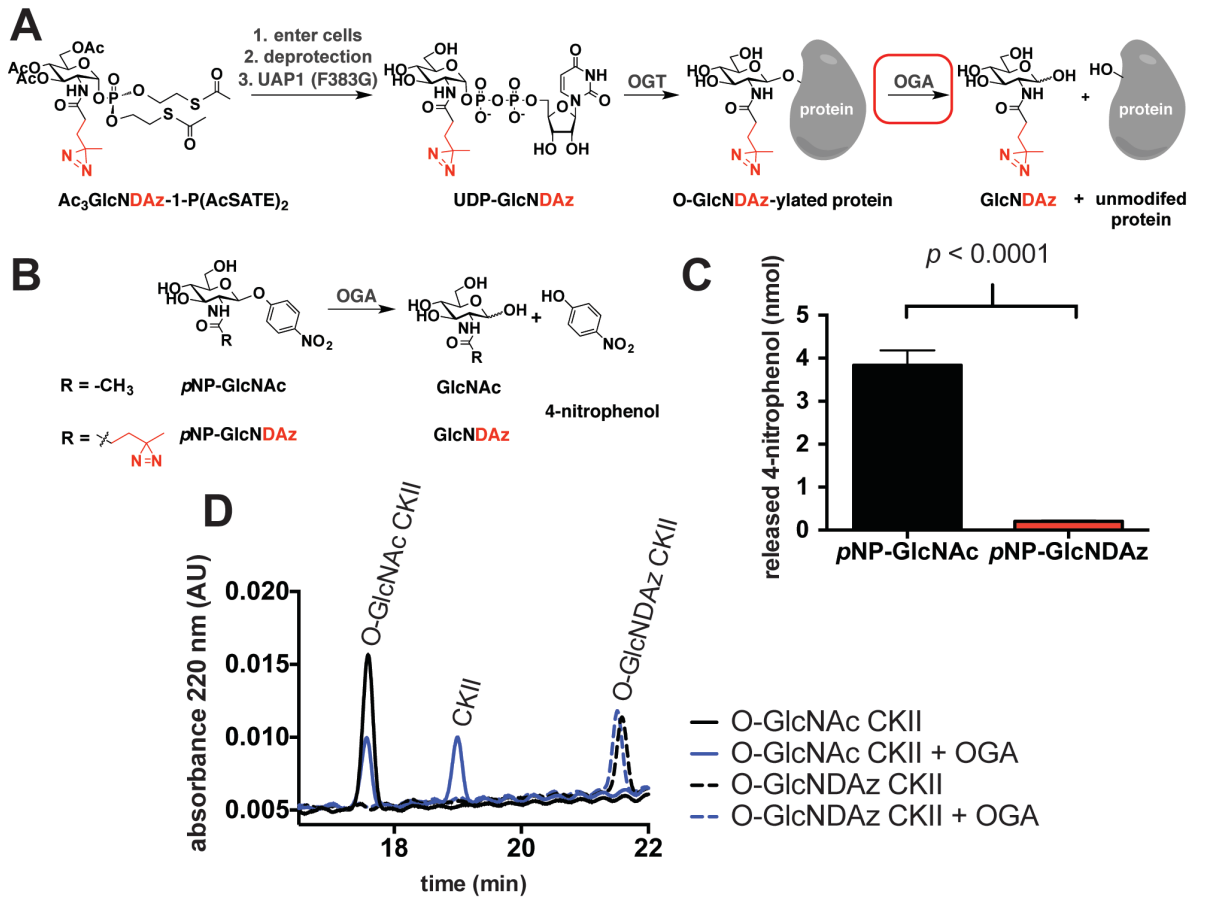

Fig. 1. OGA is inactive toward substrates containing diazirine-modified GlcNAc. (**A**) Metabolic strategy for O-GlcNDAz production. Mammalian cells are engineered to produce diazirine-modified O-GlcNAc (O-GlcNDAz) by culturing with the precursor Ac_3GlcNDAz-1-P(AcSATE)$_2$ and introducing expression of the F383G mutant of UAP1. (**B**) Para-nitrophenol derivatives of GlcNAc (*p*NP-GlcNAc) and GlcNDAz (*p*NP-GlcNDAz) serve as chromogenic substrates to monitor OGA activity. (**C**) Recombinant human OGA hydrolyzes an O-GlcNAc mimic, but not an O-GlcNDAz mimic. *p*NP-GlcNAc or *p*NP-GlcNDAz (250 μM) was incubated with OGA (50 nM). After 3 h, absorbance at 405 nm was measured to determine release of 4-nitrophenol. Error bars represent the standard deviation of three trials. (**D**) Peptide deglycosylation by wild-type OGA. O-GlcNAc- or O-GlcNDAz-modified CKII peptide was incubated with or without purified recombinant human OGA and reaction products were analyzed by HPLC. Full HPLC traces are presented in Fig. S2.

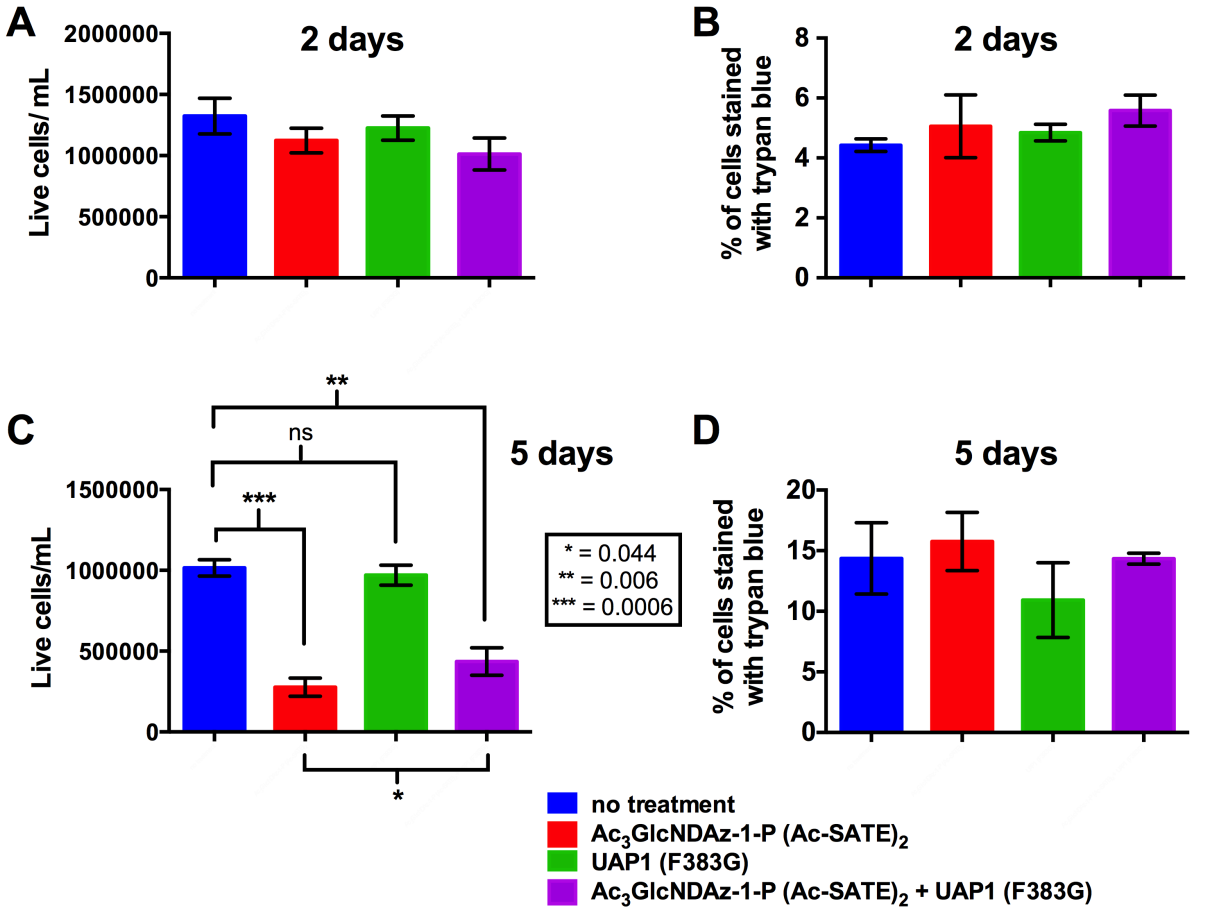

Fig. 2. O-GlcNDAz production is non-toxic. (**A**) Effect of two days of O-GlcNDAz production on cell proliferation. Parental HeLa cells or HeLa cells stably expressing UAP1(F383G) were cultured with or without Ac_3GlcNDAz-1-P$(AcSATE)_2$. After two days of O-GlcNDAz production, cells were counted. Error bars represent the standard deviation of three independent experiments. No significant differences among the conditions were detected. (**B**) Effect of two days of O-GlcNDAz production on cell viability. After two days, dead cells were stained with trypan blue and counted. Error bars represent the standard deviation of three independent experiments. No significant differences among the conditions were detected. (**C**) Effect of five days of O-GlcNDAz production on cell proliferation. Parental HeLa cells or HeLa cells stably expressing UAP1(F383G) were cultured with or without Ac_3GlcNDAz-1-P$(AcSATE)_2$. After two days of O-GlcNDAz production, cells were diluted and cultured with or without Ac_3GlcNDAz-1-P$(AcSATE)_2$ for three additional days. Then cells were counted. Error bars represent the standard deviation of three independent experiments. Addition of Ac_3GlcNDAz-1-P$(AcSATE)_2$ resulted in decreased proliferation, but this effect was partially reversed by simultaneous expression of UAP1(F383G). (**D**) Effect of five days of O-GlcNDAz production on cell viability. After five days, including one cell dilution, dead cells were stained with trypan blue and counted. Error bars represent the standard deviation of three independent experiments. No significant differences among the conditions were detected.

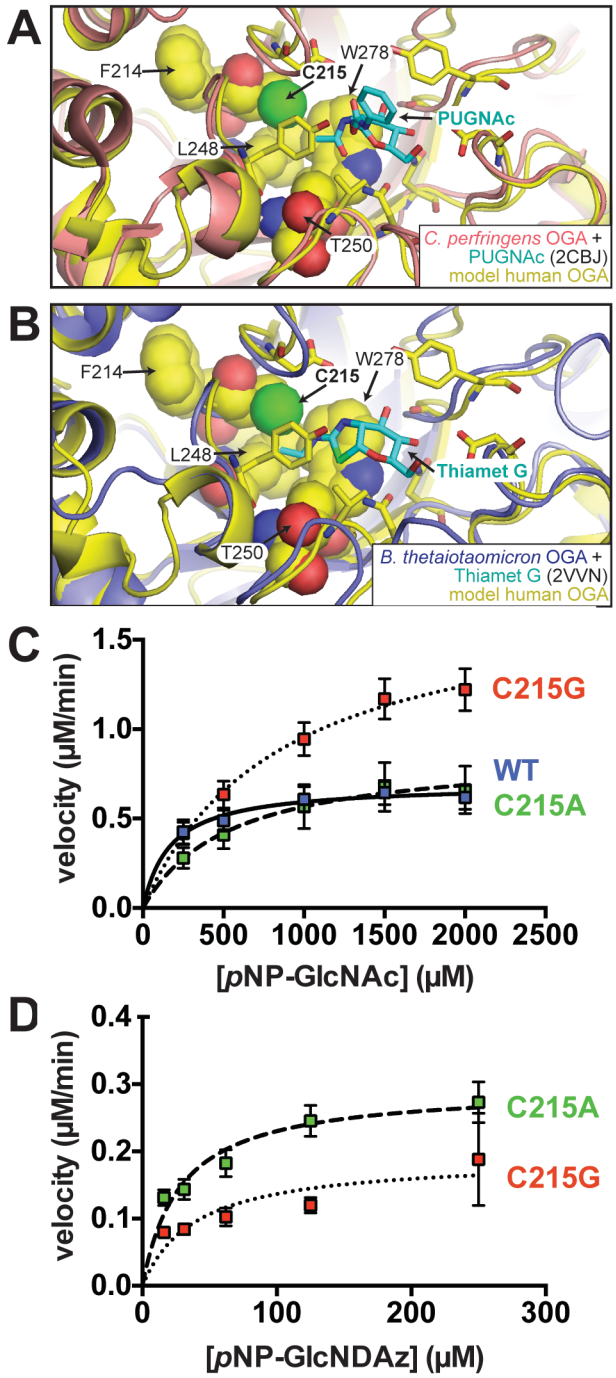

Fig. 3. Mutations to C215 of OGA restore activity toward an O-GlcNDAz mimic. (**A**) Structure of *C. perfringens* OGA complexed with PUGNAc (2CBJ; protein in pink, inhibitor in teal) aligned with a PHYRE[2]-generated model of human OGA (in yellow). Residues selected for mutation are shown in space-filling representation. (**B**) Structure of *B. thetaiotaomicron* OGA complexed with Thiamet G (2VVN; protein in blue, inhibitor in teal) aligned with the PHYRE[2]-generated model of human OGA (in yellow). Residues selected for mutation are shown in space-filling representation. (**C**) Rates of hydrolysis of *p*NP-GlcNAc by wild-type OGA, C215A mutant of OGA, and C215G mutant of OGA. (**D**) Rates of hydrolysis of *p*NP-GlcNDAz by the C215A and C215G mutants of OGA. Hydrolysis of *p*NP-GlcNDAz by wild-type OGA was too slow to be measured accurately by this approach (Fig. S5).

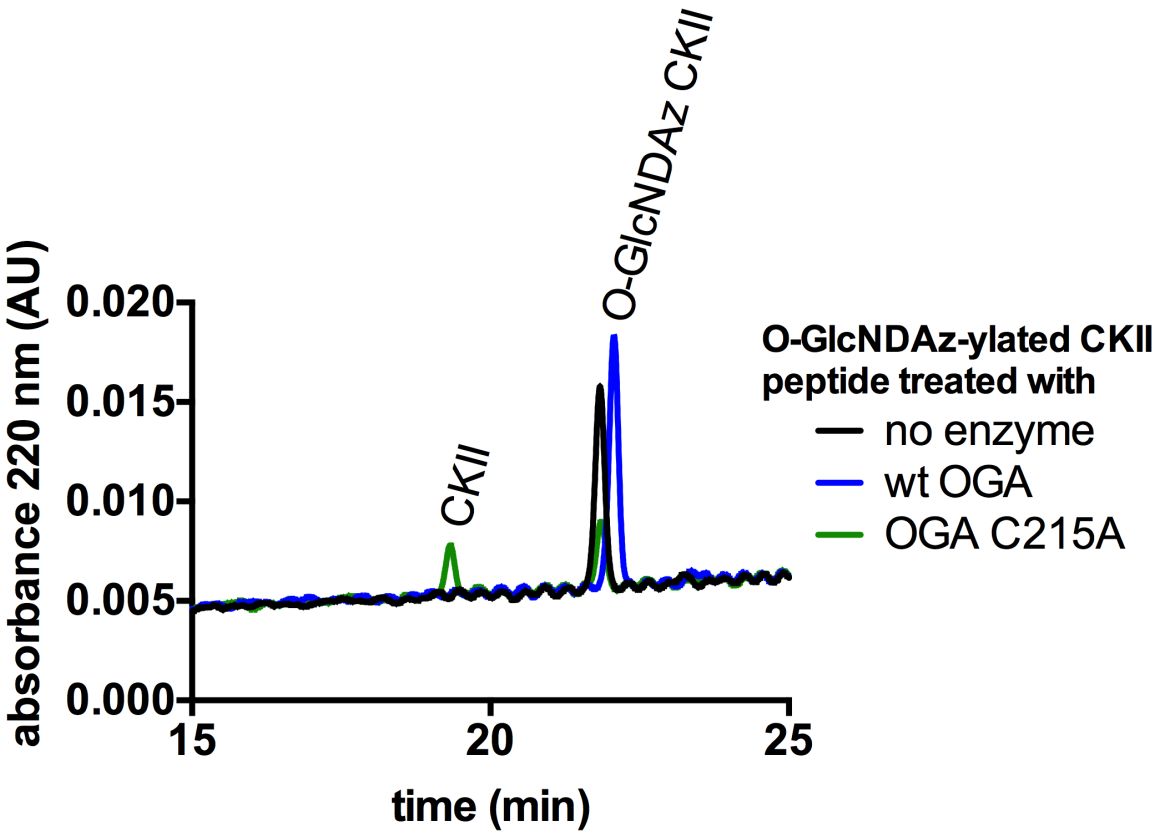

Fig. 4. C215A mutant of OGA hydrolyzes an O-GlcNDAz-modified peptide. O-GlcNDAz-ylated CKII peptide was treated with no enzyme, with wild-type OGA, or with the C215A mutant of OGA. Treatment with the C215A mutant yielded a decrease in the peak corresponding to O-GlcNDAz-ylated CKII peptide and appearance of a peak corresponding to unmodified CKII peptide. Full HPLC traces are presented in Fig. S6.

Table 1. Michaelis-Menten parameters for hydrolysis of *p*NP-GlcNAc and *p*NP-GlcNDAz by purified OGA (wild-type, C215A, and C215G).

	***p*NP-GlcNAc**			***p*NP-GlcNDAz**		
enzyme	k_{cat} **(min^{-1})**	K_m **(mM)**	k_{cat}/K_m **(mM^{-1} min^{-1})**	k_{cat} **(min^{-1})**	K_m **(mM)**	k_{cat}/K_m **(mM^{-1} min^{-1})**
wild-type	14 ± 1	0.17 ± 0.08	82 ± 40	no measurable activity		
C215A	17 ± 4	0.54 ± 0.35	32 ± 22	2.4 ± 0.2	0.03 ± 0.01	86 ± 27
C215G	36 ± 5	0.86 ± 0.30	42 ± 16	1.5 ± 0.3	0.04 ± 0.03	38 ± 29